

Room-Temperature Grafting from Synthesis of Protein–Polydisulfide Conjugates via Aggregation-Induced Polymerization

Jianhua Lu, Zhun Xu, Hailin Fu, Yao Lin, Huan Wang, and Hua Lu*



Cite This: *J. Am. Chem. Soc.* 2022, 144, 15709–15717



Read Online

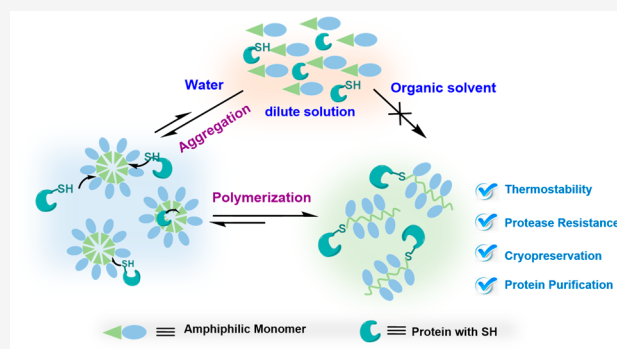
ACCESS |

Metrics & More

Article Recommendations

Supporting Information

ABSTRACT: The reversible modification of proteins with lipoic acid (LPA)-derived polydisulfides (PDS) is an important approach toward the transient regulation and on-demand recovery of protein functions. The in situ growth of PDS from the cysteine (Cys) residue of a protein, however, has been challenging due to the near-equilibrium thermodynamics of the ring-opening polymerization of LPA. Here, we report the protein-mediated, aggregation-induced polymerization (AIP) of amphiphilic LPA-derived monomers at room temperature, which can be performed at a concentration as low as ~2% of the equilibrium monomer concentration normally needed. The aggregation of monomers increases the effective monomer concentration in aqueous solutions to the degree that the polymerizations behave similarly to those in bulk. The PDS conjugation enhances the thermostability, protease resistance, and tolerance to freeze–thaw treatments of the target proteins. Moreover, the PDS conjugation allows rapid and convenient purification of Cys-bearing proteins by taking advantage of the liquid–liquid phase separation of the protein–PDS conjugates and the full recovery of native proteins under mild reducing conditions. This AIP effect may shed light on facilitating other polymerizations with a similar near-equilibrium character. The PDS conjugation can open up new avenues to protein delivery, dynamic and reversible protein engineering, enzyme preservation, and recycling.



INTRODUCTION

The ring-opening polymerization (ROP) of 1,2-dithiolanes affords polydisulfides (PDS) with fascinating self-adaptive, highly dynamic, and stimuli-responsive properties.^{1–3} Lipoic acid (LPA) and its derivatives, for example, are the most frequently studied 1,2-dithiolane monomers for their biogenesis source, intrinsic biocompatibility, and ease of modification. Although the polymerization of LPA can be traced back to as early as the 1940s, the PDS were not explicitly explored until the past decade.^{4,5} A series of pioneering works were accomplished by Matile and co-workers, who reported LPA-derived PDS with unusual thiol–disulfide exchange-mediated cellular penetration ability.^{6–10} Yao et al. have coupled various LPA-derived PDS to nanoparticles and proteins, achieving efficient cytosolic delivery of the cargos.^{11–14} Waymouth and Moore et al. have carefully studied the polymerizability of various 1,2-dithiolanes and the topology control of PDS in organic solvents, respectively.^{15,16} Moreover, Qu and Feringa et al. have together fabricated various fascinating self-healing and recyclable bulk PDS-based materials.^{17–20} Taking advantage of their unique properties of PDS, numerous new applications have been demonstrated including hydrogels, catalysis, gene delivery, etc.^{2,21–30}

One character of the ROP of 1,2-dithiolane is the full reversibility and mild conditions. We envisage that the dynamic feature of PDS can be harnessed for transient and reversible modification of proteins,³¹ achieving a broad range of sophisticated functions that are difficult to realize using conventional materials. Nevertheless, this ROP has a relatively high equilibrium monomer concentration ($[M]_{eq}$) at room temperature due to its near-equilibrium thermodynamics, i.e., a near-zero change in the Gibbs free energy ΔG_p .^{32–35} For example, the $[M]_{eq}$ of LPA in aqueous solutions is usually above 262 mM at room temperature, which is problematic for protein conjugation owing to potential precipitation of biologics.³⁶ As such, although the grafting-to synthesis of protein–PDS conjugates had been accomplished in 2015,^{8,12} the protein-mediated in situ ROP of 1,2-dithiolanes, i.e., the so-called grafting-from synthesis, was not realized until 2020 using cryo-condition.³⁶ While the more commonly used

Received: June 7, 2022

Published: August 17, 2022



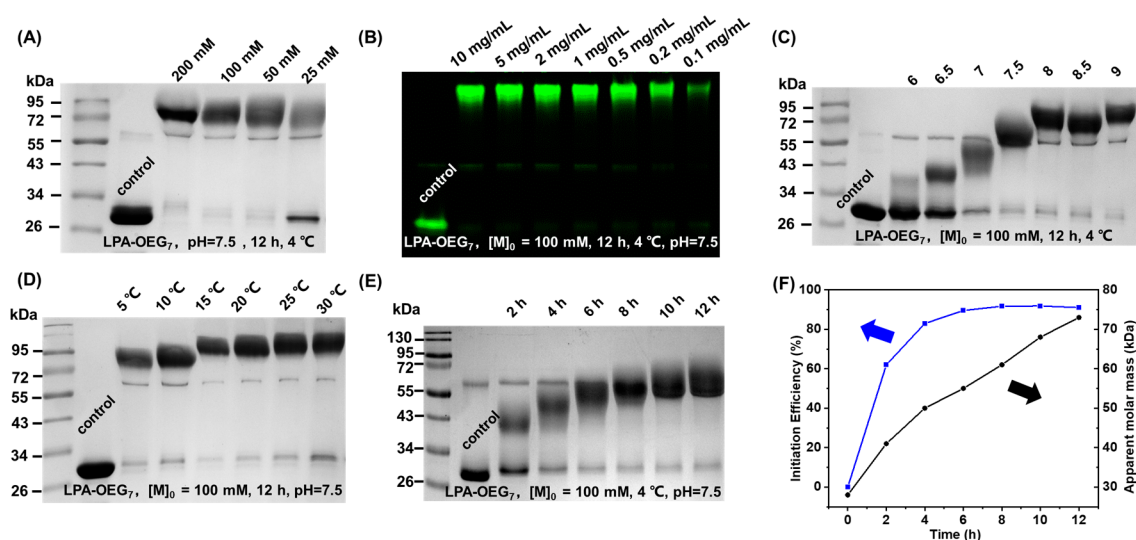


Figure 2. Optimization of EGFP-SH-mediated ROP conditions of LPA-OEG₇. (A–E) Nonreducing PAGE analysis of the ROP at various (A) monomer concentrations; (B) protein concentrations (native gel); (C) pH; (D) temperatures; (E) reaction time. (F) Plots of the initiation efficiency (blue) and apparent M_n (black) as a function of the incubation time of EGFP-SH-mediated ROP conditions of LPA-OEG₇ at 4 °C.

in the range of 1.05–1.16, suggesting good control of the ROP (Figure 1D).

We assumed the side group difference was unlikely to affect the thermodynamics of the ROP of LPA-OEG₇ and LPA in a significant way because they were far away from the 1,2-dithiolane ring. Thus, the equilibrium constants of the ROPs of LPA-OEG₇ and LPA should be comparable in the same solvent. When the temperature was fixed, the peculiarly high polymerizability of LPA-OEG₇ in aqueous solvents could only be explained by a greater effective monomer concentration $[M]_{\text{eff}}$ than the apparent $[M]_0$. Specifically, we proposed an aggregation-induced polymerization (AIP) effect for the amphiphilic LPA-OEG₇, which formed nanosized aggregates in aqueous solution and led to augmented $[M]_{\text{eff}}$ to allow successful ROP (Figure 1A). Driven by this hypothesis, we investigated the aggregation behaviors of 100 mM LPA or LPA-OEG₇ in solvents such as H₂O and DMSO using dynamic light scattering (DLS). The DLS results showed no aggregation for LPA in both solvents (deprotonated for LPA in aqueous solution, pH = 7.4); however, LPA-OEG₇ was found to form nanoparticles of ~21 nm in water but not in DMSO (Figure S2). Liquid-phase transmission electron microscopy (TEM) further confirmed the existence of droplet-like nanoparticles (aggregates) for 100 mM LPA-OEG₇ in H₂O (Figure 1E).⁴⁶ Detailed analysis found the morphology of the aggregates to be comparatively fluidic and could be easily malleable to or even completely disrupted by shear stress (Figures S3 and S4, video S1, and video S2). The critical micelle concentration (CMC) of LPA-OEG₇, measured by Nile Red encapsulation assay, was ~4 mM (Figure 1F), which roughly coincided with the minimal concentration required (~10 mM) for the ROP of LPA-OEG₇. As a comparison, no aggregation occurred for the deprotonated LPA even at 200 mM according to the same assay (Figure S5). When investigating the ROP of LPA-OEG₇ in mixed H₂O/DMSO, there was again a strong correlation between the polymerization and the formation of aggregates (Figures S2 and S6). Interestingly, varying the ROPs of LPA-OEG₇ in water at different $[M]_0$ (25–200 mM), feeding $[M]_0/[I]$ ratios (5/1–200/1), or by using different small molecular initiators,

all reached a monomer conversion $\sim 64 \pm 5\%$ (Figures S7–S9), similar to the conversion of LPA-OEG₇ ROP in bulk (Figure S10). Moreover, the ROP of LPA-OEG₇ gave a zero order kinetic character with the apparent rate constants being almost independent of $[M]_0$ (Table S2 and Figure S11), which also resembled the behaviors of bulk polymerization. Together, all these results strongly support our AIP hypothesis.

Next, we investigated whether such an AIP effect could also be observed using thiol-containing proteins as initiator, thereby facilitating the grafting-from synthesis of protein–PDS conjugates at a low $[M]_0$ and room temperature. Using an enhanced green fluorescent protein mutant bearing a reactive thiol group (EGFP-SH) as the model initiator, the conditions for the ROP of LPA-OEG₇ were optimized according to nonreducing SDS–PAGE (Figure 2). EGFP-SH was found to mediate the polymerization at a $[M]_0$ as low as 25 mM (Figure 2A), and the initiation efficiency was almost quantitative when $[M]_0$ was 50 mM or above. Unlike many bioconjugation reactions that required highly concentrated proteins, the ROP of LPA-OEG₇ was successful even at an EGFP-SH concentration of 0.1 mg/mL ($\sim 3 \mu\text{M}$) (Figure 2B and S12). Raising the buffer pH from 6.0 to 9.0 enhanced both the initiation efficiency and M_n of the final conjugates, with a plateau reached at pH ~ 8.0 (Figure 2C). Moreover, conjugates with high M_n were achievable in a broad range of biologically relevant temperatures from 5 to 30 °C (Figure 2D). Of note, the cryopolymerization of this monomer barely happened even at a $[M]_0$ of 100 mM, possibly owing to the slow kinetics caused by low temperature and the steric hindrance of the OEG₇ side group. Kinetic study results showed an almost linear growth of M_n of the conjugate over 12 h at 4 °C (Figure 2E,F), echoing the kinetics of small molecular initiator-mediated ROP (Table S2 and Figure S11) and offering a simple way for M_n control. By using a number of proteins with or without a reactive thiol for initiation, the ROP was found strictly thiol-dependent, and preexisting disulfide bonds in the protein was found nonreactive and orthogonal to the ROP under the tested conditions (see the discussion for Figure S13). Based on the above optimization results, we

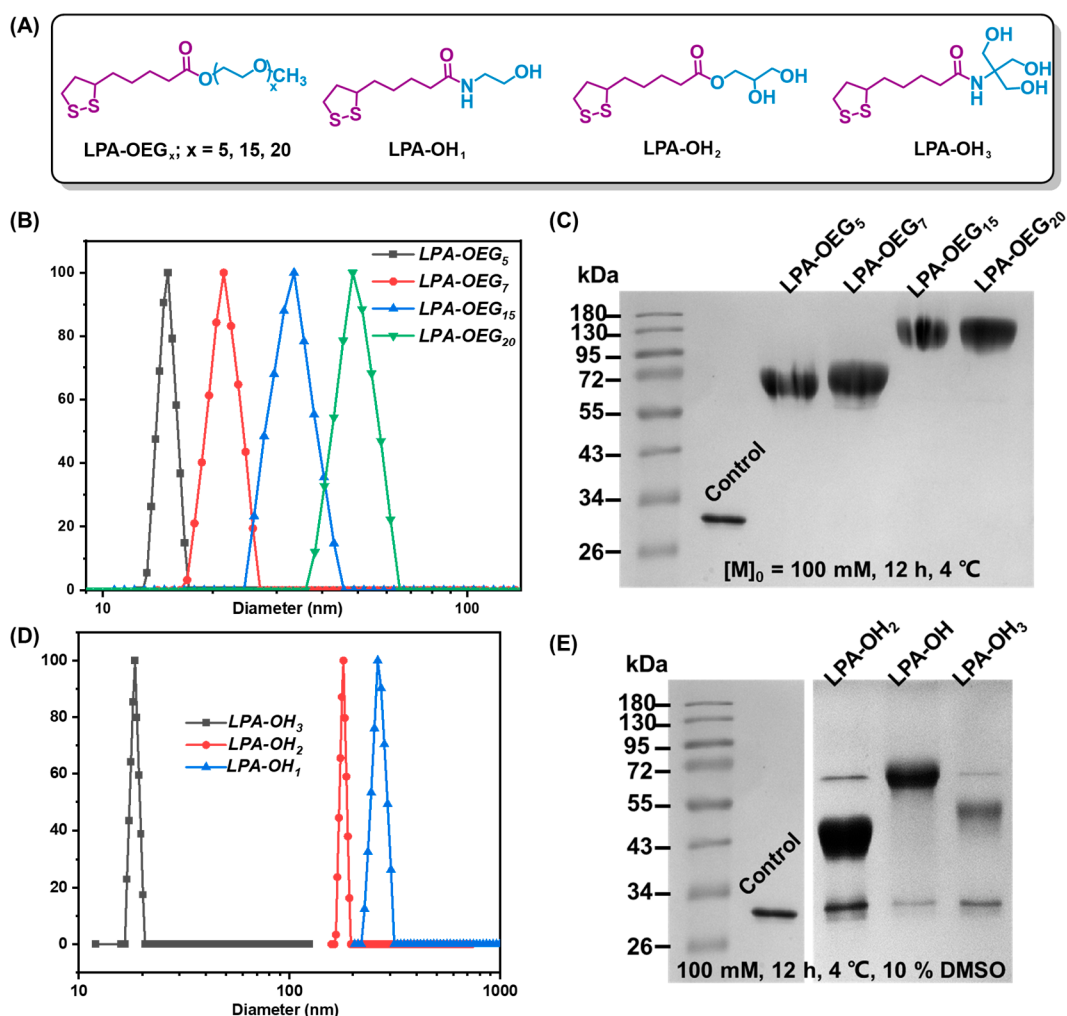


Figure 3. Monomer scope of the AIP effect. (A) Structure of monomers explored for ROP. (B) DLS and (C) nonreducing SDS–PAGE of the ROP of 100 mM LPA-OEG_x in water. (D) DLS and (E) nonreducing SDS–PAGE of the ROP of 100 mM LPA-OH_x in water containing 10% DMSO. All ROPs were initiated with EGFP-SH.

adopted $[M]_0 = 100$ mM, pH = 7.5, 4 °C, and 12 h for subsequent experiments.

We then investigated the monomer scope of the AIP effect. As shown in Figure 3A, we synthesized a series of LPA derivatives with varied lengths of methoxy oligoethylene glycol (LPA-OEG_x; $x = 5, 15, 20$). Similar to LPA-OEG₇, these monomers were all polymerizable by EGFP-SH at a $[M]_0$ of 100 mM in aqueous solutions, under which condition they all aggregated (Figure 3B,C and Figure S14). No polymerization or aggregation occurred in DMSO for the same monomers at the same concentration. We also attempted to expand the monomer scope to LPA derivatives bearing different numbers of hydroxyl groups (denoted as LPA-OH_x, where $x = 1, 2, \text{ or } 3$, respectively). Similar to the ROP results of LPA-OEG_x, LPA-OH_x also showed a strong indication of AIP in water containing 10% DMSO (Figure 3D,E). In all cases, the initiation efficiencies of EGFP-SH were ~90% or above according to the unseparated nonreducing SDS–PAGE characterization. These results collectively demonstrated that the AIP effect was generally applicable to a variety of amphiphilic 1,2-dithiolane monomers.

To interrogate how the PDS conjugation affect the structure and function of proteins, we examined the circular dichroism (CD) spectroscopy, melting temperature (T_m), proteolytic

resistance, and enzymatic activity of various protein–PDS conjugates.⁴⁷ For this, an interferon (IFN) mutant bearing genetically inserted Cys and wild type dihydrofolate reductase (DHFR) that contains native thiols were used as model proteins to mediate the ROP of LPA-OEG_x, affording the conjugates IFN-p(LPA-OEG_x) (Figure S15) and DHFR-p(LPA-OEG_x) (Figure S16), respectively. The degree of polymerization (DP) of the grafted PDS in the three IFN-p(LPA-OEG_x) conjugates ($x = 7, 15, 20$) were ~80 according to nonreducing SDS–PAGE. Thermostability was examined by first heating IFN and the three IFN-p(LPA-OEG_x) conjugates at 60 °C for 2 h followed by CD measurement. The unmodified IFN precipitated after heating and the residual protein in the supernatant failed to maintain the original secondary structure according to CD spectroscopy (Figure 4A). In contrast, IFN-p(LPA-OEG₇) preserved ~45% helicity of IFN, whereas IFN-p(LPA-OEG₁₅) and IFN-p(LPA-OEG₂₀) almost completely maintained the secondary structure of IFN under the same conditions. In accord with the CD study, the T_m values increased by 2.5–6.0 °C for the three IFN-p(LPA-OEG_x) conjugates as compared with that of IFN as revealed by the thermofluor assay (Figure 4B and S17). Modification of p(LPA-OEG_x) also significantly improved the proteolytic stability of IFN: when IFN was completely degraded within

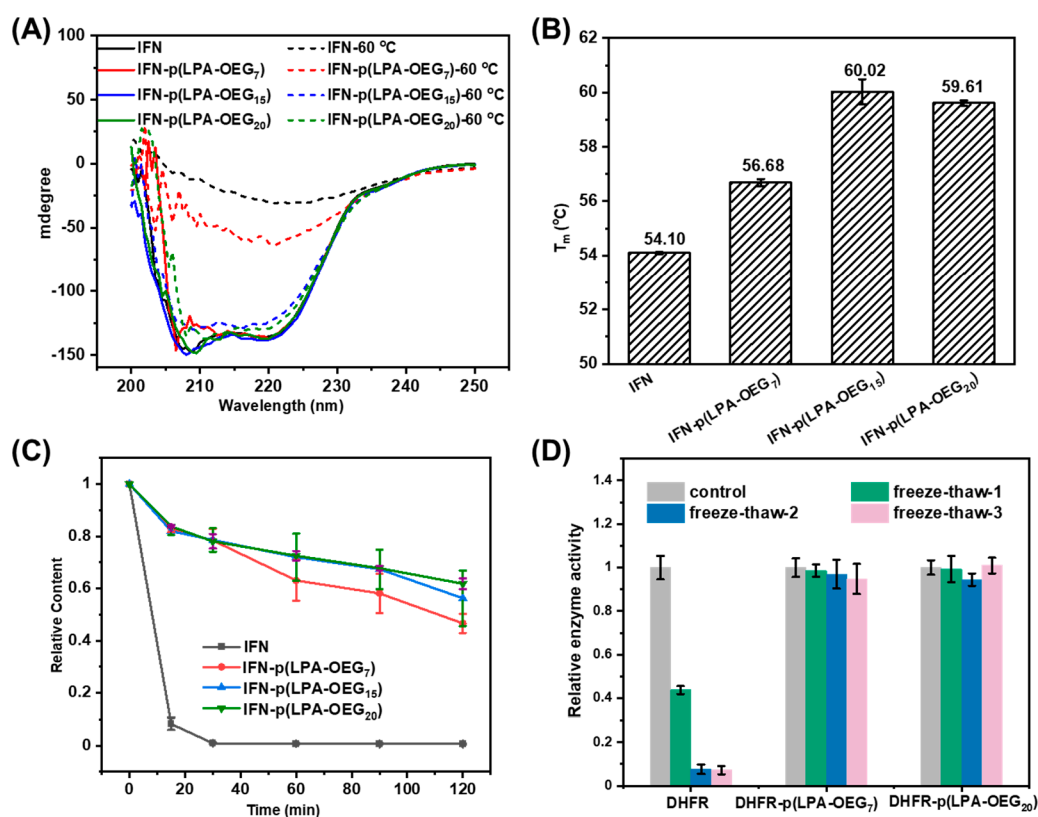


Figure 4. p(LPA-OEG_x) conjugation improved the thermostability, proteolytic resistance, and antifreeze ability of proteins. (A) CD spectra of IFN and IFN-p(LPA-OEG_x) at 25 °C (solid lines) and after heating at 60 °C for 2 h (dashed lines). (B) Melting temperature (T_m) of IFN and IFN-p(LPA-OEG_x) measured by a thermofluor assay. (C) Degradation kinetics of IFN and IFN-p(LPA-OEG_x) (0.5 mg/mL) with trypsin digestion (1 μ g/mL) at 37 °C. (D) Normalized remaining enzyme activity of DHFR and DHFR-p(LPA-OEG_x) after 1–3 freeze–thaw cycles.

30 min by trypsin, IFN-p(LPA-OEG_x) was \sim 80% and \sim 46–62% intact after incubation for 30 min and 2 h, respectively (Figure 4C and S18). Many enzymes, DHFR for instance, are vulnerable to freezing conditions, especially after repeated freeze–thaw cycles. The anti-icing and cryopreservation of those proteins are thus critically important.^{40,42,48} Indeed, after three repeated freeze–thaw cycles (from -80 °C for 12 h to room temperature), the enzymatic activity of DHFR retained only less than 10%. Remarkably, both DHFR-p(LPA-OEG₇) and DHFR-p(LPA-OEG₂₀) showed almost negligible changes in the enzyme activity after the same treatments (Figure 4D). The attachment of p(LPA-OEG₇) was also found to preserve the fluorescence of EGFP resisting photo bleaching (Figure S19).

Due to the reversibility of the ROP and the reactivity of disulfides to reductive reagents, the above-mentioned protein–PDS conjugates were expected to release native proteins under mild reducing conditions. Taking EGFP, sortase, and DHFR as examples, we made the corresponding conjugates modified with p(LPA-OEG_x) and were able to completely degrade the PDS by reducing agents (e.g., dithiothreitol (DTT), glutathione (GSH), and tris(2-carboxyethyl) phosphine (TCEP)) to recover native proteins with almost unaffected activity (Figure 5A and Figures S20 and S21). Interestingly, we found both LPA-OEG₅ and its corresponding polymer p(LPA-OEG₅) exhibited a lowest critical solution temperature (LCST) between 20 and 30 °C (Figures S22 and S23). Accordingly, the conjugate EGFP-p(LPA-OEG₅) also showed a similar LCST of \sim 30 °C (Figure 5B and Figures S24–S26) and confocal laser scanning microscopy (CLSM) demon-

strated a liquid–liquid phase separation (LLPS) of the conjugate above the LCST (Figure 5C). Taken together, the results of Figure 5A–C lead us to speculate that the ROP of LPA-OEG₅ could be harnessed to facilitate rapid separation, purification, and then recovery of thiol-bearing proteins from impurities without using expensive reagents or instruments (Figure 5D). As a proof of concept, we incubated 100 mM LPA-OEG₅ with mixed EGFP-SH and mCherry at a 1/1 mass ratio (Figure 5E, tube 1) at 4 °C for 4 h. After capping the reaction with maleimide, the solution became turbid and phase separated spontaneously upon sitting at 37 °C for 1 min. The color of the bottom and upper layers appeared yellow and magenta, respectively, suggesting good separation of EGFP-SH from mCherry (Figure 5E, tube 2). Indeed, native-PAGE of the whole reaction mixture (Figure 5E, lane 2, nonreducing) and the centrifuged bottom layer (Figure 5E, tube 3, lane 3, reducing) confirmed the EGFP-SH-selective initiation of LPA-OEG₅ and the gravity-assisted harvest of EGFP-p(LPA-OEG₅) at the bottom layer, respectively. The purity of the recovered EGFP-SH was improved from 97% to more than 99% after a single washing step of the bottom liquid phase, with a separation yield of \sim 98% (Figure 5E, Lane 4, reducing). To further showcase the high efficiency of the method, we mixed EGFP-SH with mCherry at a 1/10 mass ratio and carried out the same procedure as described above. EGFP-SH was finally obtained at \sim 90% purity and \sim 92% yield from a protein mixture in which the protein-of-interest originally accounted for only 9% (Figure 5F). Moreover, when Azor was purified by this fashion, \sim 85% of its original catalytic activity was preserved (Figure S27).

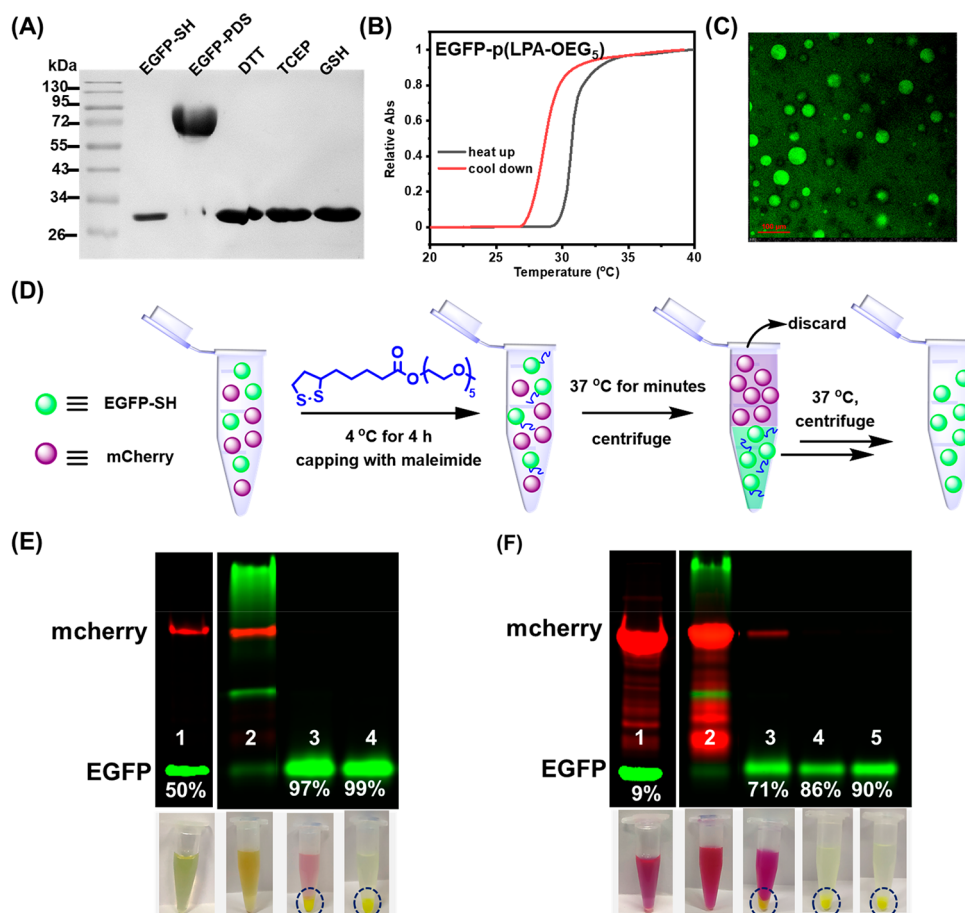


Figure 5. Facile separation and recovery of thiol-bearing proteins. (A) SDS–PAGE gel of EGFP-p(LPA-OEG₇) treated with various reducing agents. (B) Turbidity (relative absorbance at 500 nm) of EGFP-p(LPA-OEG₅) (2.0 mg/mL) as a function of temperature in water; heating or cooling ramp was at a rate of 3 °C/min. (C) CLSM of the LLPS phenomenon of EGFP-p(LPA-OEG₅) (2.0 mg/mL) at room temperature. The green color represents fluorescence of EGFP; scale bar = 100 μm. (D) Cartoon illustration of the purification principle. (E) Native-PAGE characterization (top) illustrating the purification process of EGFP-SH from mixed EGFP-SH/mCherry (1/1 mass ratio). Lane 1: EGFP-SH/mCherry mixture. Lane 2: 1 after incubating with LPA-OEG₅ at 4 °C for 4 h (nonreducing). Lane 3: bottom layer of 2 after centrifugation (reducing). Lane 4: bottom layer of 3 after washing with PBS (reducing). Below the gel are the corresponding photographs for each lane. (F) Native-PAGE characterization (top) illustrating the purification process of EGFP-SH from mixed EGFP-SH/mCherry (1/10 mass ratio). Lane 1: EGFP-SH/mCherry (1/10) mixture. Lane 2: 1 after incubating with LPA-OEG₅ at 4 °C for 4 h (nonreducing). Lane 3: bottom layer of 2 after centrifugation (reducing). Lane 4: bottom layer of 3 after washing with PBS (reducing). Lane 5: bottom layer of 3 after washing with PBS twice (reducing). Below the gel are the corresponding photographs for each lane. Nonreducing: no DTT in the loading buffer. Reducing: with DTT in the loading buffer.

In conclusion, by taking advantage of the augmented $[M]_{\text{eff}}$ originated from the aggregation of amphiphilic 1,2-dithiolanes in aqueous solutions, we realized the ROP at room temperature and under biologically benign and dilute conditions. This AIP effect allowed one-step grafting-from synthesis of various protein–PDS conjugates with high efficiency and at monomer concentrations up to 80 times lower than the equilibrium monomer concentration that was normally needed. Because a reactive thiol exists in many native proteins or obtainable using standard mutagenesis, the method avoided the hassle of complicated linker synthesis and low efficient protein–polymer ligation. In one sense, the AIP achieved a similar concentrating effect as relative to the templated polymerization,^{49,50} but in a simpler and self-templation manner. From a broader synthetic point of view, many reversible ROP systems with near-equilibrium thermodynamic characters suffered extreme conditions such as low temperatures, high viscosity, and low monomer conversion.^{35,51} Along this direction, the advantages of AIP (normal

temperatures, low concentrations, and water as solvent) may shed light on solutions on enabling and empowering the ROP of those systems beyond 1,2-dithiolanes.

Sulfur-containing polymers with versatile and dynamic properties have emerged as promising functional materials for broad applications.^{52–56} The full reversibility, along with the mild conditions to drive the backward and forward reactions, made the PDS conjugation strategy particularly attractive for transient protein regulation. We demonstrated that the in situ growth of p(LPA-OEG_x) from the surface of a protein can protect the target protein from denaturing or degrading against harsh conditions such as heat shock, protease digestion, and freeze–thaw treatments. Moreover, by utilizing the LCST and LLPS of protein–p(LPA-OEG₅) conjugates, we developed a simple and affordable method for rapid purification and recycle of thiol-bearing proteins with no need of expensive instruments or separation reagents. Compared with other LCST polymer-based protein separation methods (for example: PNIPAM or ELP), this method does

not require complicated genetic engineering or organic solvent for extraction, and can regenerate the native proteins under milder conditions in a thiol-selective way.^{57–60} The increased stability of the conjugates may facilitate and reduce cost for the transportation and storage of protein therapeutics, industrial enzymes, and vaccines. Overall, the method can open new avenues to protein delivery, dynamic and reversible regulation of protein functions, enzyme preservation, and recycling.^{12,13,61}

■ ASSOCIATED CONTENT

SI Supporting Information

The Supporting Information is available free of charge at <https://pubs.acs.org/doi/10.1021/jacs.2c05997>.

Full details of the synthesis, experimental methods, characterizations, and supporting figures (PDF)

Liquid phase TEM (AVI)

Time-lapsed change of LPA-OEG7 assembly (AVI)

■ AUTHOR INFORMATION

Corresponding Author

Hua Lu – Beijing National Laboratory for Molecular Sciences, Center for Soft Matter Science and Engineering, Key Laboratory of Polymer Chemistry and Physics of Ministry of Education, College of Chemistry and Molecular Engineering, Peking University, Beijing 100871, People's Republic of China; orcid.org/0000-0003-2180-3091; Email: chemhualu@pku.edu.cn

Authors

Jianhua Lu – Beijing National Laboratory for Molecular Sciences, Center for Soft Matter Science and Engineering, Key Laboratory of Polymer Chemistry and Physics of Ministry of Education, College of Chemistry and Molecular Engineering, Peking University, Beijing 100871, People's Republic of China

Zhun Xu – Beijing National Laboratory for Molecular Sciences, Center for Soft Matter Science and Engineering, Key Laboratory of Polymer Chemistry and Physics of Ministry of Education, College of Chemistry and Molecular Engineering, Peking University, Beijing 100871, People's Republic of China

Hailin Fu – Institute of Materials Science & Department of Chemistry, University of Connecticut, Storrs, Connecticut 06269, United States

Yao Lin – Institute of Materials Science & Department of Chemistry, University of Connecticut, Storrs, Connecticut 06269, United States; orcid.org/0000-0001-5227-2663

Huan Wang – Beijing National Laboratory for Molecular Sciences, Center for Soft Matter Science and Engineering, Key Laboratory of Polymer Chemistry and Physics of Ministry of Education, College of Chemistry and Molecular Engineering, Peking University, Beijing 100871, People's Republic of China; orcid.org/0000-0002-2542-936X

Complete contact information is available at: <https://pubs.acs.org/doi/10.1021/jacs.2c05997>

Notes

The authors declare no competing financial interest.

■ ACKNOWLEDGMENTS

This work is supported by the National Key Research and Development Program of China (2019YFA0904203) and the

National Natural Science Foundation of China (22125101). The authors would like to thank Yi Zhang for the SEC data of PDS and Prof. Yun Liu for inspiring discussion. The authors acknowledge Electron Microscopy Laboratory of Peking University, China, for the use of FEI Tecnai T20 transmission electron microscopy.

■ REFERENCES

- (1) Bang, E.-K.; Lista, M.; Sforazzini, G.; Sakai, N.; Matile, S. Poly(Disulfide)S. *Chemical Science* **2012**, *3*, 1752–1763.
- (2) Zhang, R.; Nie, T.; Fang, Y.; Huang, H.; Wu, J. Poly(Disulfide)S: From Synthesis to Drug Delivery. *Biomacromolecules* **2022**, *23*, 1–19.
- (3) Mutlu, H.; Ceper, E. B.; Li, X.; Yang, J.; Dong, W.; Ozmen, M. M.; Theato, P. Sulfur Chemistry in Polymer and Materials Science. *Macromol. Rapid Commun.* **2019**, *40*, e1800650.
- (4) Thomas, R. C.; Reed, L. J. Disulfide Polymers of DL-A-Lipoic Acid. *J. Am. Chem. Soc.* **1956**, *78*, 6148–6149.
- (5) Kishore, K.; Ganesh, K. Polymers Containing Disulfide, Tetrasulfide, Diselenide and Ditelluride Linkages in the Main-Chain. *Adv. Polym. Sci.* **1995**, *121*, 81–121.
- (6) Bang, E. K.; Gasparini, G.; Molinard, G.; Roux, A.; Sakai, N.; Matile, S. Substrate-Initiated Synthesis of Cell-Penetrating Poly-(Disulfide)S. *J. Am. Chem. Soc.* **2013**, *135*, 2088–2091.
- (7) Bang, E.-K.; Ward, S.; Gasparini, G.; Sakai, N.; Matile, S. Cell-Penetrating Poly(Disulfide)S: Focus on Substrate-Initiated Copolymerization. *Polym. Chem.* **2014**, *5*, 2433–2441.
- (8) Gasparini, G.; Matile, S. Protein Delivery with Cell-Penetrating Poly(Disulfide)S. *Chem. Commun.* **2015**, *51*, 17160–17162.
- (9) Gasparini, G.; Bang, E. K.; Molinard, G.; Tulumello, D. V.; Ward, S.; Kelley, S. O.; Roux, A.; Sakai, N.; Matile, S. Cellular Uptake of Substrate-Initiated Cell-Penetrating Poly(Disulfide)S. *J. Am. Chem. Soc.* **2014**, *136*, 6069–6074.
- (10) Pulcu, G. S.; Galenkamp, N. S.; Qing, Y.; Gasparini, G.; Mikhailova, E.; Matile, S.; Bayley, H. Single-Molecule Kinetics of Growth and Degradation of Cell-Penetrating Poly(Disulfide)S. *J. Am. Chem. Soc.* **2019**, *141*, 12444–12447.
- (11) Du, S.; Liew, S. S.; Zhang, C. W.; Du, W.; Lang, W.; Yao, C. C. Y.; Li, L.; Ge, J.; Yao, S. Q. Cell-Permeant Bioadaptors for Cytosolic Delivery of Native Antibodies: A "Mix-and-Go" Approach. *ACS Cent. Sci.* **2020**, *6*, 2362–2376.
- (12) Fu, J.; Yu, C.; Li, L.; Yao, S. Q. Intracellular Delivery of Functional Proteins and Native Drugs by Cell-Penetrating Poly-(Disulfide)S. *J. Am. Chem. Soc.* **2015**, *137*, 12153–12160.
- (13) Qian, L.; Fu, J.; Yuan, P.; Du, S.; Huang, W.; Li, L.; Yao, S. Q. Intracellular Delivery of Native Proteins Facilitated by Cell-Penetrating Poly(Disulfide)S. *Angew. Chem., Int. Ed.* **2018**, *57*, 1532–1536.
- (14) Yu, C.; Qian, L.; Ge, J.; Fu, J.; Yuan, P.; Yao, S. C.; Yao, S. Q. Cell-Penetrating Poly(Disulfide) Assisted Intracellular Delivery of Mesoporous Silica Nanoparticles for Inhibition of Mir-21 Function and Detection of Subsequent Therapeutic Effects. *Angew. Chem., Int. Ed.* **2016**, *55*, 9272–9276.
- (15) Zhang, X.; Waymouth, R. M. 1,2-Dithiolane-Derived Dynamic, Covalent Materials: Cooperative Self-Assembly and Reversible Cross-Linking. *J. Am. Chem. Soc.* **2017**, *139*, 3822–3833.
- (16) Liu, Y.; Jia, Y.; Wu, Q.; Moore, J. S. Architecture-Controlled Ring-Opening Polymerization for Dynamic Covalent Poly(Disulfide)-S. *J. Am. Chem. Soc.* **2019**, *141*, 17075–17080.
- (17) Zhang, Q.; Shi, C. Y.; Qu, D. H.; Long, Y. T.; Feringa, B. L.; Tian, H. Exploring a Naturally Tailored Small Molecule for Stretchable, Self-Healing, and Adhesive Supramolecular Polymers. *Sci. Adv.* **2018**, *4*, eaat8192.
- (18) Zhang, Q.; Deng, Y. X.; Luo, H. X.; Shi, C. Y.; Geise, G. M.; Feringa, B. L.; Tian, H.; Qu, D. H. Assembling a Natural Small Molecule into a Supramolecular Network with High Structural Order and Dynamic Functions. *J. Am. Chem. Soc.* **2019**, *141*, 12804–12814.

- (19) Zhang, Q.; Qu, D. H.; Feringa, B. L.; Tian, H. Disulfide-Mediated Reversible Polymerization toward Intrinsically Dynamic Smart Materials. *J. Am. Chem. Soc.* **2022**, *144*, 2022–2033.
- (20) Zhang, Q.; Deng, Y.; Shi, C.-Y.; Feringa, B. L.; Tian, H.; Qu, D.-H. Dual Closed-Loop Chemical Recycling of Synthetic Polymers by Intrinsically Reconfigurable Poly(Disulfides). *Matter* **2021**, *4*, 1352–1364.
- (21) Zhou, J.; Sun, L.; Wang, L.; Liu, Y.; Li, J.; Li, J.; Li, J.; Yang, H. Self-Assembled and Size-Controllable Oligonucleotide Nanospheres for Effective Antisense Gene Delivery through an Endocytosis-Independent Pathway. *Angew. Chem., Int. Ed.* **2019**, *58*, S236–S240.
- (22) Zhu, Y.; Lin, M.; Hu, W.; Wang, J.; Zhang, Z. G.; Zhang, K.; Yu, B.; Xu, F. J. Controllable Disulfide Exchange Polymerization of Polyguanidine for Effective Biomedical Applications by Thiol-Mediated Uptake. *Angew. Chem., Int. Ed.* **2022**, e202200535.
- (23) Wang, H.; Hu, Y.; Wang, Y.; Lu, J.; Lu, H. Doxorubicin@Pepylated Interferon-Polydisulfide: A Multi-Responsive Nanoparticle for Enhanced Chemo–Protein Combination Therapy. *Giant* **2021**, *5*, 100040–100047.
- (24) Michal, B. T.; Jaye, C. A.; Spencer, E. J.; Rowan, S. J. Inherently Photohealable and Thermal Shape-Memory Polydisulfide Networks. *ACS Macro Lett.* **2013**, *2*, 694–699.
- (25) Huang, C. H.; Nwe, K.; Al Zaki, A.; Brechbiel, M. W.; Tsourkas, A. Biodegradable Polydisulfide Dendrimer Nanoclusters as MRI Contrast Agents. *ACS Nano* **2012**, *6*, 9416–9424.
- (26) Agergaard, A. H.; Sommerfeldt, A.; Pedersen, S. U.; Birkedal, H.; Daasbjerg, K. Dual-Responsive Material Based on Catechol-Modified Self-Immobilized Poly(Disulfide) Backbones. *Angew. Chem., Int. Ed.* **2021**, *60*, 21543–21549.
- (27) Huang, S.; Shen, Y.; Bisoyi, H. K.; Tao, Y.; Liu, Z.; Wang, M.; Yang, H.; Li, Q. Covalent Adaptable Liquid Crystal Networks Enabled by Reversible Ring-Opening Cascades of Cyclic Disulfides. *J. Am. Chem. Soc.* **2021**, *143*, 12543–12551.
- (28) Trzcinski, J. W.; Morillas-Becerril, L.; Scarpa, S.; Tannorella, M.; Muraca, F.; Rastrelli, F.; Castellani, C.; Fedrigo, M.; Angelini, A.; Tavano, R.; Papini, E.; Mancini, F. Poly(Lipoic Acid)-Based Nanoparticles as Self-Organized, Biocompatible, and Corona-Free Nanovectors. *Biomacromolecules* **2021**, *22*, 467–480.
- (29) Yu, N.; Zhang, Y.; Li, J.; Gu, W.; Yue, S.; Li, B.; Meng, F.; Sun, H.; Haag, R.; Yuan, J.; Zhong, Z. Daratumumab Immunopolymer-some-Enabled Safe and Cd38-Targeted Chemotherapy and Depletion of Multiple Myeloma. *Adv. Mater.* **2021**, *33*, e2007787.
- (30) Chen, C. J.; Ng, D. Y. W.; Weil, T. Polymer Bioconjugates: Modern Design Concepts toward Precision Hybrid Materials. *Prog. Polym. Sci.* **2020**, *105*, 101241–101280.
- (31) Gong, Y.; Leroux, J. C.; Gauthier, M. A. Releasable Conjugation of Polymers to Proteins. *Bioconjugate Chem.* **2015**, *26*, 1172–1181.
- (32) Houk, J.; Whitesides, G. M. Characterization and Stability of Cyclic Disulfides and Cyclic Dimeric Bis(Disulfides). *Tetrahedron* **1989**, *45*, 91–102.
- (33) Burns, J. A.; Whitesides, G. M. Predicting the Stability of Cyclic Disulfides by Molecular Modeling: Effective Concentrations in Thiol-Disulfide Interchange and the Design of Strongly Reducing Dithiols. *J. Am. Chem. Soc.* **1990**, *112*, 6296–6303.
- (34) Endo, K.; Yamanaka, T. Copolymerization of Lipoic Acid with 1,2-Dithiane and Characterization of the Copolymer as an Interlocked Cyclic Polymer. *Macromolecules* **2006**, *39*, 4038–4043.
- (35) Coates, G. W.; Getzler, Y. D. Y. L. Chemical Recycling to Monomer for an Ideal, Circular Polymer Economy. *Nat. Rev. Mater.* **2020**, *5*, 501–516.
- (36) Lu, J.; Wang, H.; Tian, Z.; Hou, Y.; Lu, H. Cryopolymerization of 1,2-Dithiolanes for the Facile and Reversible Grafting-from Synthesis of Protein-Polydisulfide Conjugates. *J. Am. Chem. Soc.* **2020**, *142*, 1217–1221.
- (37) Pincock, R. E. Reactions in Frozen Systems. *Acc. Chem. Res.* **1969**, *2*, 97–103.
- (38) Takenaka, N.; Bandow, H. Chemical Kinetics of Reactions in the Unfrozen Solution of Ice. *J. Phys. Chem. A* **2007**, *111*, 8780–8786.
- (39) Anzo, K.; Harada, M.; Okada, T. Enhanced Kinetics of Pseudo First-Order Hydrolysis in Liquid Phase Coexistent with Ice. *J. Phys. Chem. A* **2013**, *117*, 10619–10625.
- (40) Mancini, R. J.; Lee, J.; Maynard, H. D. Trehalose Glycopolymers for Stabilization of Protein Conjugates to Environmental Stressors. *J. Am. Chem. Soc.* **2012**, *134*, 8474–8479.
- (41) Lee, J.; Lin, E. W.; Lau, U. Y.; Hedrick, J. L.; Bat, E.; Maynard, H. D. Trehalose Glycopolymers as Excipients for Protein Stabilization. *Biomacromolecules* **2013**, *14*, 2561–2569.
- (42) Mitchell, D. E.; Fayter, A. E. R.; Deller, R. C.; Hasan, M.; Gutierrez-Marcos, J.; Gibson, M. I. Ice-Recrystallization Inhibiting Polymers Protect Proteins against Freeze-Stress and Enable Glycerol-Free Cryostorage. *Mater. Horiz.* **2019**, *6*, 364–368.
- (43) Li, B.; Wu, Y.; Zhang, W.; Zhang, S.; Shao, N.; Zhang, W.; Zhang, L.; Fei, J.; Dai, Y.; Liu, R. Efficient Synthesis of Amino Acid Polymers for Protein Stabilization. *Biomater. Sci.* **2019**, *7*, 3675–3682.
- (44) Fayter, A. E. R.; Hasan, M.; Congdon, T. R.; Kontopoulou, I.; Gibson, M. I. Ice Recrystallization Inhibiting Polymers Prevent Irreversible Protein Aggregation During Solvent-Free Cryopreservation as Additives and as Covalent Polymer-Protein Conjugates. *Eur. Polym. J.* **2020**, *140*, 110036.
- (45) Uyeda, H. T.; Medintz, I. L.; Jaiswal, J. K.; Simon, S. M.; Mattoussi, H. Synthesis of Compact Multidentate Ligands to Prepare Stable Hydrophilic Quantum Dot Fluorophores. *J. Am. Chem. Soc.* **2005**, *127*, 3870–3878.
- (46) Nagamanasa, K. H.; Wang, H.; Granick, S. Liquid-Cell Electron Microscopy of Adsorbed Polymers. *Adv. Mater.* **2017**, *29*, 1703555–1703560.
- (47) Hou, Y.; Yuan, J.; Zhou, Y.; Yu, J.; Lu, H. A Concise Approach to Site-Specific Topological Protein-Poly(Amino Acid) Conjugates Enabled by in Situ-Generated Functionalities. *J. Am. Chem. Soc.* **2016**, *138*, 10995–11000.
- (48) Liu, Z.; Zheng, X.; Wang, J. Bioinspired Ice-Binding Materials for Tissue and Organ Cryopreservation. *J. Am. Chem. Soc.* **2022**, *144*, 5685–5701.
- (49) Laurent, Q.; Sakai, N.; Matile, S. An Orthogonal Dynamic Covalent Chemistry Tool for Ring-Opening Polymerization of Cyclic Oligochalcogenides on Detachable Helical Peptide Templates. *Chem.—Eur. J.* **2022**, *28*, e202200785.
- (50) Niu, J.; Hili, R.; Liu, D. R. Enzyme-Free Translation of DNA into Sequence-Defined Synthetic Polymers Structurally Unrelated to Nucleic Acids. *Nat. Chem.* **2013**, *5*, 282–292.
- (51) Olsen, P.; Odelius, K.; Albertsson, A. C. Thermodynamic Presynthetic Considerations for Ring-Opening Polymerization. *Biomacromolecules* **2016**, *17*, 699–709.
- (52) Tian, T.; Hu, R.; Tang, B. Z. Room Temperature One-Step Conversion from Elemental Sulfur to Functional Polythioureases through Catalyst-Free Multicomponent Polymerizations. *J. Am. Chem. Soc.* **2018**, *140*, 6156–6163.
- (53) Zhang, J.; Zang, Q.; Yang, F.; Zhang, H.; Sun, J. Z.; Tang, B. Z. Sulfur Conversion to Multifunctional Poly(O-Thiocarbamate)S through Multicomponent Polymerizations of Sulfur, Diols, and Diisocyanides. *J. Am. Chem. Soc.* **2021**, *143*, 3944–3950.
- (54) Yuan, J.; Xiong, W.; Zhou, X.; Zhang, Y.; Shi, D.; Li, Z.; Lu, H. 4-Hydroxyproline-Derived Sustainable Polythioesters: Controlled Ring-Opening Polymerization, Complete Recyclability, and Facile Functionalization. *J. Am. Chem. Soc.* **2019**, *141*, 4928–4935.
- (55) Xiong, W.; Chang, W.; Shi, D.; Yang, L.; Tian, Z.; Wang, H.; Zhang, Z.; Zhou, X.; Chen, E.-Q.; Lu, H. Geminal Dimethyl Substitution Enables Controlled Polymerization of Penicillamine-Derived B-Thiolactones and Reversed Depolymerization. *Chem.* **2020**, *6*, 1831–1843.
- (56) Zhang, X.-H.; Theato, P. *Sulfur-Containing Polymers: From Synthesis to Functional Materials*; Wiley-VCH: Weinheim, 2021.
- (57) Meyer, D. E.; Trabbic-Carlson, K.; Chilkoti, A. Protein Purification by Fusion with an Environmentally Responsive Elastin-Like Polypeptide: Effect of Polypeptide Length on the Purification of Thioredoxin. *Biotechnol. Prog.* **2001**, *17*, 720–728.

(58) Kanazawa, H.; Nishikawa, M.; Mizutani, A.; Sakamoto, C.; Morita-Murase, Y.; Nagata, Y.; Kikuchi, A.; Okano, T. Aqueous Chromatographic System for Separation of Biomolecules Using Thermoresponsive Polymer Modified Stationary Phase. *J. Chromatogr. A* **2008**, *1191*, 157–161.

(59) Baker, S. L.; Munasinghe, A.; Kaupbayeva, B.; Rebecca Kang, N.; Certiat, M.; Murata, H.; Matyjaszewski, K.; Lin, P.; Colina, C. M.; Russell, A. J. Transforming Protein-Polymer Conjugate Purification by Tuning Protein Solubility. *Nat. Commun.* **2019**, *10*, 4718–4729.

(60) Sweet, C.; Aayush, A.; Readnour, L.; Solomon, K. V.; Thompson, D. H. Development of a Fast Organic Extraction-Precipitation Method for Improved Purification of Elastin-Like Polypeptides That Is Independent of Sequence and Molecular Weight. *Biomacromolecules* **2021**, *22*, 1990–1998.

(61) Mackenzie, K. J.; Francis, M. B. Recyclable Thermoresponsive Polymer-Cellulase Bioconjugates for Biomass Depolymerization. *J. Am. Chem. Soc.* **2013**, *135*, 293–300.

Recommended by ACS

Propagation-Instigated Self-Limiting Polymerization of Multiarmed Amphiphiles into Finite Supramolecular Polymers

Hao Su, Honggang Cui, *et al.*

OCTOBER 29, 2021
JOURNAL OF THE AMERICAN CHEMICAL SOCIETY

READ 

Oxidative Polymerization in Living Cells

Yiheng Dai, Huaping Xu, *et al.*

JUNE 23, 2021
JOURNAL OF THE AMERICAN CHEMICAL SOCIETY

READ 

Programming Self-Assembly and Stimuli-Triggered Response of Hydrophilic Telechelic Polymers with Sequence-Encoded Hydrophobic Initiators

Adrian Moreno, Gerard Lligadas, *et al.*

AUGUST 18, 2020
MACROMOLECULES

READ 

Heterochiral β -Peptide Polymers Combating Multidrug-Resistant Cancers Effectively without Inducing Drug Resistance

Ning Shao, Runhui Liu, *et al.*

APRIL 14, 2022
JOURNAL OF THE AMERICAN CHEMICAL SOCIETY

READ 

Get More Suggestions >